The First Singlet (n,π^*) and (π,π^*) Excited States of the Hydrogen-Bonded Complex between Water and Pyridine

Zheng-Li Cai and Jeffrey R. Reimers*

School of Chemistry, The University of Sydney, NSW 2006, Australia

Received: February 27, 2002

The excited-state hydrogen bonding between a pyridine molecule and a water molecule has been investigated by a series of theoretical methods including direct and time-dependent density functional theory (DFT and TD-DFT), complete-active-space self-consistent-field (CASSCF) with second-order perturbation-theory correction (CASPT2), and equation-of-motion coupled-cluster (EOM-CCSD). All calculations indicate that the water:pyridine complex on the ground state has strong hydrogen-bonding with binding enthalpies ranging from 4.5 to 5.9 kcal mol^{-1} after basis set superposition error, zero-point, and thermal correction, with the water molecule lying perpendicularly to the pyridyl plane (total C_s symmetry for the complex). This is in reasonable agreement with experiment and also with previous DFT and MP2 (second-order Møller−Plesset perturbation theory) calculations with large basis sets. Similar results are obtained for hydrogen bonding to the lowest (π,π^*) excited state, S_2 ($^1B_2$). However, for this complex in its first (n-π^*) state, S_1 ($^1B_1$), pyridine is found to adopt a boat configuration of only C_s symmetry with the water above the pyridyl plane. Both the EOM-CCSD and CASPT2 calculations indicate that reasonably strong hydrogen-bonding occurs to pyridine in the (n-π^*) state, with the calculated bond enthalpies ranging from 4.0 to 4.5 kcal mol^{-1}. Hence, we find that excited-state hydrogen bonding to azines remains important, but that it has a *different motif* from the usual linear hydrogen bonding found in ground-state systems. For the (n,π^*) excited state, the hydrogen bonding is to the electron-enhanced π cloud of the aromatic ring. A new, much more complex picture is presented for hydrogen bonding in azines which is qualitatively consistent with observed spectroscopic data.

1. Introduction

Hydrogen bonding is very important in the molecular sciences as it plays a central role in the structure and function of all biological systems,[1−3] and hydrogen bonding involving azines and their derivatives such as nucleobases is particularly significant. Most of our knowledge concerns hydrogen bonding to molecules in their ground electronic state; these have been widely investigated by different spectroscopic methods,[4−13] and characteristic bond energies, structures, and vibrational frequencies have been obtained. Much less is know about hydrogen bonding to molecules in excited states, however. Archetypal studies include the absorption and fluorescence studies which culminated in the work of Baba, Goodman, and Valenti,[4] supersonic molecular jet spectroscopy pioneered by Bernstein et al.,[14,15] and computations pioneered by Del Bene.[16−19] The (n,π^*) states are particularly pertinent as the electronic transition removes one of the lone-pair electrons that directly participate in the hydrogen bonding. The properties of (π,π^*) excited states are also relevant to proton-transfer and tautomerization in azines.[20,21]

The basic concepts involved were elucidated in 1965 by Baba, Goodman, and Valenti,[4] who studied the absorption and fluorescence spectra of pyridine and the diazines (pyridazine, pyrimidine, and pyrazine) in dilute solution in a variety of hydrogen-bonding and non-hydrogen-bonding solvents. They found that in hydrogen-bonding solvents the hydrogen bond that is formed between the solute in its ground electronic state and solvent molecules gives rise to a large blue shift in the (n,π^*) absorption transition but only small changes in the corresponding fluorescence spectrum. Dielectric solvation theories[22−25] express these solvent shifts as

$$\Delta U = -\frac{2\epsilon - 2}{2\epsilon + 1}\frac{1}{a^3}\mu_i(\mu_f - \mu_i) - \frac{n^2 - 1}{2n^2 + 1}\frac{1}{a^3}|\mu_f - \mu_i|^2 \quad (1)$$

where μ_i and μ_f are the dipole moment vectors of the initial and final states solvated outside a cavity of radius a by a material of dielectric constant ϵ and refractive index n. As the coefficient of the first term is much larger than that for the second and as only the first term can give rise to a blue shift, Baba et al. qualitatively interpreted the experimental data as indicating a large dipole moment (ca. 3 D) the ground state and a nearly zero dipole moment in the excited state. From this, they concluded that the hydrogen bonding is broken in the (n,π^*) singlet excited state of pyridine and the diazines. Their analysis appears quite valid for pyridine, but for the diazines, it is incomplete as it does not properly address the issue of the localization/delocalization of the (n,π^*) excitation over the two nitrogen atoms. In the ground state, liquid-structure simulations indicate that two hydrogen bonds are formed to the diazines.[26−29] In the excited state, if the excitation localizes onto one nitrogen atom, then this atom becomes analogous to the nitrogen in pyridine, whereas the other atom is unaffected. One would thus expect that the hydrogen bond to the unaffected nitrogen would remain intact, whereas the other hydrogen bond would break. However, if the excitation is delocalized over both diazine nitrogen atoms, then each atom will have 1.5 electrons with which it may form hydrogen bonds to its environment, and it is not clear a priori whether hydrogen bonds are likely to

* To whom correspondence should be addressed.

10.1021/jp020552z CCC: $22.00
Published on Web 08/15/2002

form.[28−30] Before the effects of through-bond interactions were known, strong interactions between nitrogen lone-pairs were not expected, and thus, the excitations in pyrimidine and pyrazine (at least) were believed to be localized excitations,[28] even for uncomplexed pyrazine.[31] For pyrazine, however, the experimental results of Baba et al. do not support the idea of localized excitation as this would guarantee a large change in dipole moment between the excited and ground states, and high-resolution spectroscopy clearly indicates that the (n,π^*) excitation is delocalized in isolated pyrazine.[28]

Wanna, Menapace, and Bernstein[14,15] have studied the hydrogen bonded and van der Waals clusters of pyridazine, pyrazine, pyrimidine, and benzene (solutes) with C_nH_{2n+2}, NH_3, and H_2O (solvents) by the techniques of supersonic molecular jet spectroscopy and two-color time-of-flight mass spectroscopy. They did not observe pyridazine, pyrazine, or pyrimidine water clusters, however, and concluded that the excited states of these clusters must be dissociative; an alternative option raised by the present work is discussed in the conclusions section, however. Stable excited states have indeed been observed for a range of other azine complexes with hydrogen-bond donors.[32]

The hydrogen-bonding between azines in their ground electronic states and water have been investigated computationally many times,[1,7,10−13,28−30,33−41] but only Del Bene[16−19] has studies excited-state hydrogen bonding in these systems. These studies involved the evaluation of vertical excitation energies and revealed that for pyridine the additional excitation energy supplied to the hydrogen-bonded complex as a consequence of the "blue shift" of the absorption band slightly exceeded the ground-state hydrogen-bond energy. As a result, water:pyridine is expected to directly dissociate following (n,π^*) excitation. However, the calculated blue shift for diazines and some substituted pyridines was less than that required for direct dissociation, suggesting that stable excited-state complex could be obtained after excitation. To improve this analysis, the calculation of 0−0 transition energies by the most reliable means currently available is required.

The structure of a hydrogen bond to an (n,π^*) excited state in the gas phase has only been investigated in detail for the HF:H_2CO complex by Del Bene at al.[42] They found a distinctly different motif for hydrogen bonding in the excited state to normal ground-state motifs. It is not clear a priori if hydrogen bonding to aromatic (n,π^*) excited states will display similar or different motifs to that found for HF:H_2CO.

In aqueous solution, the electronic and geometrical structure of pyridine and the diazines in (n,π^*) excited states have been simulated by Zeng, Hush, and Reimers.[25−30,43] Both the nature of the hydrogen bonding and calculated solvent shifts are found to be very sensitive to the details of the potential-energy surfaces used, particularly in regard to the treatment of the localization/delocalization of the (n,π^*) excitation. They found poor agreement between experiment and results predicted using localized excitation models. Delocalized models predicted that the hydrogen bonding is considerably weakened in the excited state, but on average, one hydrogen bond remains intact to a diazine. The predicted solvent shifts were qualitatively in agreement with the experimental observations of Baba et al.,[4] though improved quantitative accuracy is required. Of particular significance was their observation that the excited-state hydrogen bonding gave rise to structures in the liquid more like those found in van der Waals bonded systems than those typical of hydrogen bonding. In particular, their potential-energy surfaces for the diazine−water clusters displayed minima in which the water molecule sat above the aromatic ring, offering simultaneous hydrogen-bond-type interactions with the azine nitrogens *and* the electron-enhanced aromatic π cloud. The presence of bound structures of this type could provide an alternate explanation of the observations of Wanna, Menapace, and Bernstein.[14] They closely resemble structures found in benzene and fluorobenzene complexes with water (see, for example, refs 14, 38, and 44−46).

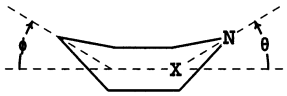

Figure 1. "Boat" distortion of S_1 ($^1B_1$), the lowest (n,π^*) state of pyridine.

Here, we will study the structures, bond energies, and vibration frequencies of water:pyridine in its ground and first-excited (n,π^*) and (π,π^*) states. Chemically, the interactions of pyridine with water are much simpler than those for the diazines, and this study thus serves as a check that modern computational methods can make sensible predictions for the properties of excited-state hydrogen bonds. We use analogous methods for both the ground and excited states. In particular, we use density functional theory (DFT) and time-dependent DFT[47−52] (TD-DFT) using the B3LYP[53] and BLYP[54,55] functionals, second-order Møller−Plesset perturbation theory[56] (MP2), complete-active-space self-consistent-field[57] (CASSCF) with second-order perturbation-theory correction[58] (CASPT2), coupled-cluster theory[59] (CCSD), and equation-of-motion coupled-cluster[60] (EOM-CCSD) theory. This work is based on our recent comprehensive treatise of the excited-state manifolds of isolated pyridine[61] in which we consider in detail energetics, structure, and vibrational motion; it embodies the results of a large range of experimental[18,62−73] and computational[36,47,61,70,72,74−78] studies. Of particular relevance, we investigated in detail the "boat" distortion (see Figure 1) of the lowest singlet state, the (n,π^*) state S_1 and the analogous triplet state $^3B_1$, providing the first assignment of the high-resolution singlet to triplet absorption spectrum and the low-resolution phosphoresence spectrum of the molecule. The singlet state has a double-well structure in the b_1 mode 16b which produces the "boat" distortion, but it is of insufficient depth to support zero-point vibration, and hence, the molecule appears to retain C_{2v} symmetry after excitation.

2. Computational Details

All TD-DFT calculations were performed by TURBOMOLE[79] using the "M3" integrating grid and the energy convergence criterion set to 10^{-10} au, with all derivatives evaluated numerically in internal coordinates using our own program. Computationally efficient auxiliary basis sets[80] were used for all TD-BLYP calculations, facilitating excited-state geomety optimization. Direct DFT geometry optimizations and frequency calculations were performed for the grouund-state with the aid of analytical derivatives using Gaussian 98.[81] The CCSD[59] and EOM-CCSD[60] calculations were performed using analytical first derivatives by ACES-II.[82] CASSCF geometry optimizations were performed typically using DALTON,[83] but sometimes MOLCAS[84] or MOLPRO.[85] CASSCF harmonic frequency calculations were performed using the analytical derivatives available in the DALTON[83] package. Only single-point energy calculations were performed at the CASPT2 level, using the MOLCAS[84] package. All available MP2 calculations were performed using GAUSSIAN 98.[81]

The basis sets used for geometry optimizations are Dunning's correlation-consistent polarized valence double- and triple-ζ

TABLE 1: Comparison of Calculated and Experimental Properties of Water in Its Ground State and Pyridine in Its $^1A_1$ Ground State (GS) and S_1 (n,π^*) and S_2 (π,π^*) Excited States

		RMS error in property								
		bond length/Å		bond angle/°		frequency[a]/cm^{-1}				
							pyridine			pyridine (n,π^*)
method	basis	water	pyridine GS	water	pyridine GS	water	GS	S_1	S_2	16b well depth[b]/cm^{-1}
SCF	cc-pVDZ	0.007	0.007	0.09	0.27	12	36			
SCF	aug-cc-pVDZ	0.014		1.41		34				
CASSCF	cc-pVDZ	0.003	0.002	0.18	0.38	36	37	82	25	90
CASSCF	aug-cc-pVDZ	0.005		1.32		33				
CASSCF[e]	6-31G**		0.008		0.29		34			
MP2	cc-pVDZ	0.007	0.012	2.62	0.31	17	30			320[c]
MP2	aug-cc-pVDZ	0.008		0.74		41				
MP2	cc-pVTZ	0.001		1.12						
CCSD	cc-pVDZ	0.007	0.012	2.34	0.27	10	23	72[d]	37[d]	140[d]
CCSD	aug-cc-pVDZ	0.007		0.36		24				
BLYP	cc-pVDZ	0.022	0.016	2.71	0.21	19	21			0[h]
BLYP	aug-cc-pVDZ	0.017		0.37		22				
B3LYP	cc-pVDZ	0.011	0.007	1.78	0.07	42	23			0[f]
B3LYP	aug-cc-pVDZ	0.007		0.23		23				
B3LYP[g]	cc-pVTZ		0.003		0.19		17			

[a] Using scale factors[92] of 0.9434, 0.91, 0.95, 0.9614, 0.9945, and 0.8935 for MP2, CASSCF, CCSD, B3LYP, BLYP, and SCF, respectively. [b] Observed[64] 4 cm^{-1}. [c] CASPT2 from ref 61 evaluated at EOM-CCSD optimized geometries. [d] EOM-CCSD from ref 61. [e] From ref 72. [f] TD-B3LYP from ref 61. [g] From ref 76. [h] TD-BLYP from ref 61.

basis sets cc-pVDZ and cc-pVTZ;[86] energetics are considered at these optimized geometries using the augmented basis sets aug-cc-pVDZ, aug-cc-pVTZ,[87] and aug-cc-pVQZ.[87] However, for the excited states considered, cc-pVDZ and aug-cc-pVDZ are the largest practicable basis sets.

Interaction energies ΔE for the complex AB are calculated using various treatments of the basis set superposition error (BSSE). For aug-cc-pVTZ basis sets and larger, it is known that use of the counterpoise correction[88,89] does not improve calculated energies,[90,91] but such corrections are required for cc-pVDZ, however. Most of our calculations are performed using aug-cc-pVDZ, and for this, we demonstrate that the best results are obtained using fractional correction. Binding enthalpies are obtained from these interaction energies by the addition of thermal and zero-point vibrational energy (ZPE) corrections obtained using the harmonic approximation, with calculated frequencies scaled by factors[92] of 0.9434 for MP2, 0.95 for CCSD and EOM-CCSD, 0.91 for CASSCF, 0.9614 for B3LYP, and 0.9945 for BLYP.

The CASSCF and CASPT2 calculations were performed using an active space[61] consisting of 8 electrons (2 lone pair, 6 π) distributed in 11 orbitals ($5a_1$, $2a_2$, and $4b_1$). This is sufficiently large to guarantee the continuity of the potential-energy surface of pyridine on displacement from its C_{2v} ground-state equilibrium geometry in modes of b_1 symmetry. It is inadequate for a_2 and b_2 distortions, but these are not of great interest herein. Intricies concerning the design of active spaces for calculations on pyridine have been described elsewhere.[61] The active space is not modified for use with water:pyridine as the included pyridine orbitals lie well within the band gap of water and there is no direct involvement of water orbitals in the spectroscopic transitions studied.

3. Results and Discussion

Only a limited number of methods are available for excited-state geometry optimizations and frequency calculations, and computational feasibility significantly limits the size of the basis sets which may be applied. Before considering such calculations, we first examine the properties of the isolated pyridine and water monomers, and the properties of ground-state water:pyridine, verifying that the methods that we employ for the excited states in fact provide useful descriptions of these simpler systems. For reference, all ground and excited-state monomer and complex optimized geometries, vibration frequencies, and normal modes are provided in detail in Supporting Information.

3.1. Pyridine and Water Monomers. In Table 1 are shown the root-mean-square (RMS) differences between experimental[62,93,94] structural parameters and vibrational frequencies of water and of pyridine in their $^1A_1$ ground states (GS) and those calculated at the MP2, CASSCF, CCSD, B3LYP, and BLYP levels with the cc-pVDZ and aug-cc-pVDZ basis. Full details of these results are provided in the Supporting Information. Results from recent, possibly more extensive calculations are also shown in Table 1 for comparison, whereas a more exhaustive and detailed survey is also available elsewhere.[61] In summary, all computed results are in good agreement with experiment; no significant improvement in the results is associated with expansion of the basis set beyond cc-pVDZ.

Also shown in Table 1 are results for the lowest (n,π^*) state, S_1 ($^1B_1$), and the lowest (π,π^*) state, S_2 ($^1B_2$). For these, the CASPT2, CASSCF, EOM-CCSD, TD-B3LYP, and TD-BLYP methods were used. The only available geometrical experimental data is the rotational constants of S_1, and these are reproduced adequately by our CASSCF and EOM-CCSD optimized geometries.[61] A total of six vibrational modes have been experimentally assigned[62] for S_1 and four for S_2, and the RMS errors in the CASSCF and EOM-CCSD calculated frequencies are provided. These errors are typically double those for the ground state. This arises because the most apparent modes in the spectrum are often ones which are strongly vibronically active; vibronically active modes have significantly different frequencies in the ground and excited states, and the frequency shift is very sensitive to small errors in perceived excited-state energy gaps.

Of particular interest is mode 16b which is observed at 406 cm^{-1} in the ground state[62] and 58 cm^{-1} in S_1, the excited-state[64] potential being interpreted as containing a double-minimum of depth 4 cm^{-1}. CASSCF, EOM-CCSD, and CASPT2 predict double-minimum potential-energy surfaces, but the calculated well depths, which are also shown in Table 1, are significantly larger indicating that these methods slightly overestimate the

TABLE 2: Calculated (cc-pVDZ Basis Set) and Observed Vertical (E_v) and Adiabatic (E_0) Excitation Energies for the First Two Singlet (n,π^*) States, S_1 ($^1B_1$) and S_3 ($^1A_2$), and the First (π,π^*) State, S_2 ($^1B_2$), of Pyridine, in eV[a]

	E_v			E_0		
method	S_1	S_3	S_2	S_1	S_3	S_2
CASSCF	5.68	6.37	5.2	5.11	5.59	4.95
CASPT2	5.00	5.25	4.89	4.45[b]	4.40[b]	4.56[b]
EOM-CCSD	5.29	5.69	5.29	4.80	4.84	5.11
TD-BLYP	4.39	4.44	5.29	3.96	3.74	5.10
TD-B3LYP	4.83	5.09	5.58	4.40	4.31	5.41
obs.[c]	4.90	5.52	5.13	4.47		4.90

[a] All geometries are taken from ref 61. [b] At the EOM-CCSD optimized geometry. [c] Vertically, this is the average band absorption energy rather than simply just the band maximum; all energies are corrected for zero-point energy, see Table 3 and ref 61.

strength of the vibronic coupling; TD-BLYP and TD-B3LYP do not predict double-minima[61] and hence clearly underestimate the vibronic coupling. Although the calculated (and observed) well depths are too shallow to support zero-point motion, the magnitude of the geometrical distortions is quite large. For S_1, the calculated torsional angles (θ, φ), as defined in Figure 1, are (27°, 9°) by EOM-CCSD and (33°, 12°) by CASSCF; for the analogous triplet state $^3B_1$, the same distortion occurs, but the well is very much deeper,[61] and the observed[95] distortion angles are (40°, 10°), whereas the calculated values are (41°, 12°) by CCSD, (2°, 12°) by CASSCF, (38°, 10°) by B3LYP, and (37°, 9°) by BLYP. The CASSCF value of $\theta = 2°$ for $^3B_1$ is clearly anomalous and arises from surface continuity problems specific to $^3B_1$ and arises from use of an overly restricted active space. Nevertheless, substantial out-of-plane displacements for S_1 are indicated.

Shown in Table 2 are calculated and observed vertical and adiabatic excitation energies for not only the S_1 ($^1B_1$) and S_2 ($^1B_2$) states of pyridine but also for the additional low-lying (n,π^*) state S_3 ($^1A_2$). Although it is usual to approximate the observed vertical excitation energy from the frequency of the absorption maximum, in quantitative studies, it is important to obtain the best possible estimate of the average absorption energy and values are available for pyridine.[61] Also, the computed values need to be corrected for zero-point energy changes, but this is not feasible for all of the computational methods used. Our approach is therefore to determine "best estimated" zero-point energy changes using the computational methods for which this is feasible to evaluate. All computed zero-point energy changes are shown in Table 3, where our best-estimate values are defined. We apply this correction to the observed vertical excitation energies shown in Table 2 in order to obtain a direct comparison with the raw calculated values. Both the zero-point energy correction and the difference between the vertical excitation energy and the band-maximum energy are large compared with anticipated accuracy of modern computational methods; hence, in quantitative studies, their inclusion is essential.

Experimentally, the S_1 (n,π^*) and S_2 (π,π^*) states are observed vertically just 0.23 eV apart, with the (n,π^*) state being the lowest in energy; this gap increases to 0.43 eV adiabatically. The CASPT2, EOM-CCSD, and CASSCF methods underestimate these gaps, whereas TD-B3LYP and TD-BLYP overestimate them. Other computational methods such as STEOM[78] and EOM-CCSD(T)[77] are known to give more accurate absolute energies than the methods used, but unfortunately, these are not feasible for water:pyridine. In this application, the relative energy changes associated with molecular distortion are perhaps more important than the absolute energies, and we have shown[61] that CASPT2, EOM-CCSD, and TD-B3LYP all provide excellent descriptions of the excited-state surfaces of pyridine within the region of interest.

One significant feature is that all of the computational methods used underestimate the vertical energy gap between the two (n,π^*) states S_1 and S_3 and predict that S_3 is adiabatically either near-degenerate with S_1 or lower in energy. Unfortunately, the origin of S_3, a single-photon forbidden state, has not been observed, but as calculations[61] place the conical intersection of S_1 and S_3 in the Franck−Condon region, the origin of S_3 is believed to lie at least 0.2 eV above that of S_1. On solvation, it is possible that S_3 is preferentially solvated compared to S_1 and hence forms the lowest-energy excited state of the complex. Henceforth, we assume that this is not the case and that S_1 remains lower in energy. Later, we calculate that upon solvation S_1 remains of lower energy than the lowest (π,π^*) state, S_2.

3.2. Ground State of Water:Pyridine. This hydrogen-bonded complex has been the subject of many investigations[1,7,10−13,30,33−41] and its basic structure and energetics are known. As our interest is in vibrational analyses and excited states, we employ more approximate methods than have otherwise been used. Results are provided in Tables 4 (comparison of calculated energies for some particular structures) and 5 (key structural and energetic information), Figure 2 (optimized structures), and the Supporting Information (complete listing of structures, energies, vibrational frequencies, and normal modes). In total, we consider five possible structures for the complex: two bifurcated structures with C_{2v} symmetry and the water molecule located either planar or perpendicular to the pyridine, known as C_{2v}(planar) and C_{2v}(perp), two analogous single hydrogen-bonded structures with C_s symmetry, known as C_s(planar) and C_s(perp), and one which is a modification of the C_s(perp) structure having C_1 symmetry. These five structures, optimized using CASSCF, are depicted in Figure 2; those as optimized by other methods are quite similar and hence not explicitly shown.

Calculated hydrogen-bond interaction energies ΔE, evaluated at the CASSCF-optimized coordinates for the five structures considered, are shown in Table 4, along with results from previous calculations. As the hydrogen-bonding topologies are quite varied, appropriate treatment of basis-set superposition error (BSSE) is required in order to be able to properly compare the energies of different structures. For small basis sets, especially those not including augmented functions such as cc-pVDZ, inclusion of corrections for BSSE is essential, whereas for aug-cc-pVTZ and larger bases, results closer to the complete-basis-set (CBS) limit are obtained without correction.[90,91] The MP2 calculations shown in Table 4 were designed to find the optimum treatment of BSSE for water:pyridine using the largest practicable basis set for the excited-state calculations, aug-cc-pVDZ. They show the calculated ground-state interaction energies evaluated using cc-pVDZ, aug-cc-pVDZ, aug-cc-pVTZ, and aug-cc-pVQZ, with and without the BSSE correction applied for aug-cc-pVDZ. Also shown are the results from the aug-cc-pVXZ series extrapolated using[96−98]

$$E(\mathrm{CBS}) = E(\mathrm{X}) - \frac{c_4}{(X+0.5)^4} - \frac{c_6}{(X+0.5)^6} \qquad (2)$$

Alternative extrapolation schemes such as Dunning's inverse 3rd and 5th power formula[90] produce very similar results. From the table, it is clear that the bindings calculated in the CBS limit lie approximately midway between the raw aug-cc-pVDZ results and those as corrected for BSSE. We hence introduce

TABLE 3: Calculated Changes in Zero-Point Energy upon Complex Formation or Excitation

	pyridine + water → water:pyridine							
	$^1A_1$ GS		S_1 (n,π^*)	S_2 (π,π^*)	GS C_s(perp) → S_1 C_s(top)		GS C_s(perp) → S_2 C_s(perp)	
method	C_s(planar)	C_s(perp)	C_s(top)	C_s(perp)	pyridine	water:pyridine	pyridine	water:pyridine
CASSCF/eV	0.086[a]	0.092[a]	0.074	0.061[a]	−0.14	−0.17	−0.11	−0.14
MP2/eV	0.066	0.078[a]						
CCSD[b]/eV		0.089[a]	0.089	0.082[a]	−0.18	−0.18	−0.16	−0.18
BLYP[c]/eV		0.078[a]						
B3LYP[d]/eV		0.080[a]						
best est./eV	0.076	0.083	0.082	0.072	−0.16	−0.18	−0.14	−0.16
(kcal mol^{-1})	(1.75)	(1.91)	(1.89)	(1.66)	(−3.7)	(−4.2)	(−3.2)	(−3.7)

[a] Ignoring one intermolecular vibration of imaginary frequency. [b] EOM-CCSD for excited states. [c] TD-BLYP for excited states. [d] TD-B3LYP for excited states.

TABLE 4: Calculated Interaction Energies ΔE, in kcal mol^{-1}, for Water to the Ground State of Pyridine, Evaluated at Consistent (Not Necessarily Fully Optimized) Sets of Geometries as a Function of Basis-Set Expansion[a]

	CASSCF[b]		MP2[c]							CASPT2[b]		CCSD[b]		BLYP[d]		B3LYP[b]	
structure	VDZ + BSSE	aVDZ	VDZ + BSSE	VTZ + BSSE	aVDZ + BSSE	aVDZ	aVTZ	aVQZ	CBS	VDZ + BSSE	aVDZ	VDZ + BSSE	aVDZ	VDZ + BSSE	aVDZ	VDZ + BSSE	aVDZ
C_{2v}(planar)	−1.20	−0.80	−2.04	−2.34	−2.49	−3.34	−3.01	−2.89	−2.80	−0.62	−2.51	−1.76	−2.74	−1.41	−1.84	−1.44	−1.79
C_{2v}(perp)	−1.60	−2.06	−2.34	−3.03	−3.37	−4.32	−4.05	−3.91	−3.80	−1.48	−3.43	−2.22	−3.73	−1.76	−2.50	−2.05	−2.65
C_s(planar)[e]	−11.16	−7.05	−4.41	−5.47	−5.85	−6.99	−6.79	−6.58	−6.40	−1.98	−5.98	−3.92	−6.46	−3.50	−5.15	−3.96	−5.33
C_s(perp)[f]	−10.50	−8.85	−4.42	−5.71	−6.11	−7.44	−7.19	−5.97	−6.78	−2.57	−6.33	−4.32	−6.61	−4.16	−5.93	−4.52	−5.76
C_1	−8.95		−3.85	−5.24	−5.42	−6.90	−6.64			−2.30		−4.01		−3.39	−4.59	−4.14	−5.22
ave. BSSE	2.05	0.40	3.66	1.84	1.17	1.17	0.59		-	2.90	0.86	2.81	0.97	4.16	0.46	2.89	0.43
max. BSSE	2.53	0.53	5.34	2.53	1.48	1.48	0.74		-	4.11	0.96	3.94	1.29	5.98	0.56	4.05	0.46

[a] Using basis sets: VDZ- cc-pVDZ, aVDZ- aug-cc-pVDZ, VTZ- cc-pVTZ, aVTZ- aug-cc-pVTZ, and aVQZ- aug-cc-pVQZ; CBS is the extrapolated[96−98] complete basis set limit. [b] At CASSCF/cc-pVDZ geometry. [c] At MP2/cc-pVDZ geometry. [d] At BLYP/cc-pVDZ geometry. [e] −4.622 kcal/mol at the SCF/STO-3G level.[17] [f] −4.549 kcal/mol at the SCF/STO-3G level;[17] −5.98 kcal/mol at the SCF/4-31G** level;[34] −5.31 to − 8.23 kcal/mol at the SCF, MP2, and DFT/DZP levels;[36] −6.23 to −6.98 kcal/mol at OPLS-AA and MP2 levels;[33] −5.43 and −7.59 kcal/mol at the SCF/6-31+G** and MP2/6-31+G** levels, respectively;[7] −6.28 and −6.08 kcal/mol at the MP2/aug-cc-pVDZ and B3LYP/aug-cc-pVDZ levels, respectively;[41] −6.15 and −6.03 kcal/mol at the MP2/6-31+G(d+,p) and B3LYP/6-31+G(d+,p) levels, respectively[1]; −6.44 kcal/mol at the MP2/6-31G(d,p) level.[38]

TABLE 5: Calculated Interaction Energies[a] ΔE and Key Calculated Geometric Parameters for the Electronic States of Water:Pyridine

			ΔE/kcal mol^{-1}											
state	structure	geometry	native	CASPT2	CCSD[b]	B3LYP[c]	$R_{N,O}$/Å	$R_{N,H}$/Å	$R_{C4,O}$/Å	$R_{C4,H}$/Å	∠NHO/°	∠XNH/°	θ/°	φ/°
GS	C_s(perp)	CASSCF	−8.57	−5.84	−6.06	−5.56	3.084	2.137	5.881	6.105	172.8	177.3	0.1	0.0
		MP2	−6.76				2.946	1.979	5.770	5.939	172.0	178.1	0.1	0.0
		CCSD	−7.04	−6.14	−7.04	−6.24	2.980	2.015	5.785	5.959	172.3	178.9	0.0	0.0
		BLYP	−5.68	−6.61	−6.51	−5.57	2.925	1.943	5.747	5.892	170.6	179.3	0.0	0.0
		B3LYP	−6.38	−5.95	−6.66	−6.38	2.916	1.944	5.715	5.886	171.3	178.9	0.0	0.0
(n,π^*)	C_{2v} (perp)	CASSCF	0.52	−0.45	−1.14	0.42	3.107	2.637	5.803	5.278	111.1	163.5	0	0
		TD-BLYP	−2.30	6.11	7.45	3.91	2.289	1.845	5.101	4.550	103.1	154.8	0	0
	C_{2v} (planar)	TD-BLYP	3.25	3.27	3.55	7.45	2.448	2.028	5.266	4.751	103.2	180	0	0
	C_s (top)	CASSCF	−9.10	−4.28	−4.41	−0.62	3.243	2.301	3.876	3.436	171.6	98.7	34.3	12.3
		EOM-CCSD	−5.70	−5.16	−5.70	−1.46	3.142	2.226	3.456	2.764	157.7	106.1	30.4	10.2
		TD-BLYP	−1.50	−3.63	−3.84	−0.47	3.410	2.643	3.295	2.394	135.3	89.4	13.3	12.0
(π,π^*)	C_s(perp)	CASSCF	−6.57	−5.53	−6.29	−5.47	3.088	2.142	6.010	6.237	172.7	176.6	0.1	0.2
		EOM-CCSD	−5.97	−6.44	−5.97	−3.94	2.991	2.033	5.930	6.059	168.5	177.1	0	0

[a] Calculated using the aug-cc-pVDZ basis set with fractional corrections for BSSE at geometries optimized using cc-pVDZ. [b] EOM-CCSD for excited states. [c] TD-B3LYP for excited states.

the fractional BSSE correction

$$E_{\text{fract}} = E_{\text{raw}} + \lambda E_{\text{BSSE}} \tag{3}$$

and optimize the fraction λ to be 0.51. Also shown in Table 4 are CASSCF, CASPT2, CCSD, BLYP, and B3LYP energies evaluated using the cc-pVDZ and aug-cc-pVDZ basis sets and the associated BSSE corrections. They indicate that the manifestations of BSSE are qualitatively similar for all computational methods to those discussed in detail for MP2. Hence, in all tables after Table 4, all binding energies are evaluated only using the aug-cc-pVDZ basis set using the fractional BSSE correction scheme of eq 3.

All computational methods considered indicate that the C_s(perp) structure has the lowest energy, in agreement with the results of previous calculations.[1,7,17,33,34,36,38,41] For it, the hydrogen-bond strengths $-\Delta E$ shown in Table 5 evaluated at the MP2, CASPT2, B3LYP, BLYP, and CCSD levels with the aug-cc-pVDZ range from 5.6 to 7.0 kcal mol^{-1} after fractional BSSE correction. The observed[99] enthalpy of formation of water:pyridine doubly dilute in CCl_4 is $\Delta H = -4.1 \pm 0.4$ kcal mol^{-1}; to compare to this, the calculated binding energies must be corrected for zero-point motion and finite temperature. The best-estimate zero-point energy correction from Table 3 is 1.8 kcal mol^{-1}, and the corresponding thermal correction is −0.7 kcal mol^{-1} so that the calculated value is $\Delta H = -4.5$ to −5.9 kcal

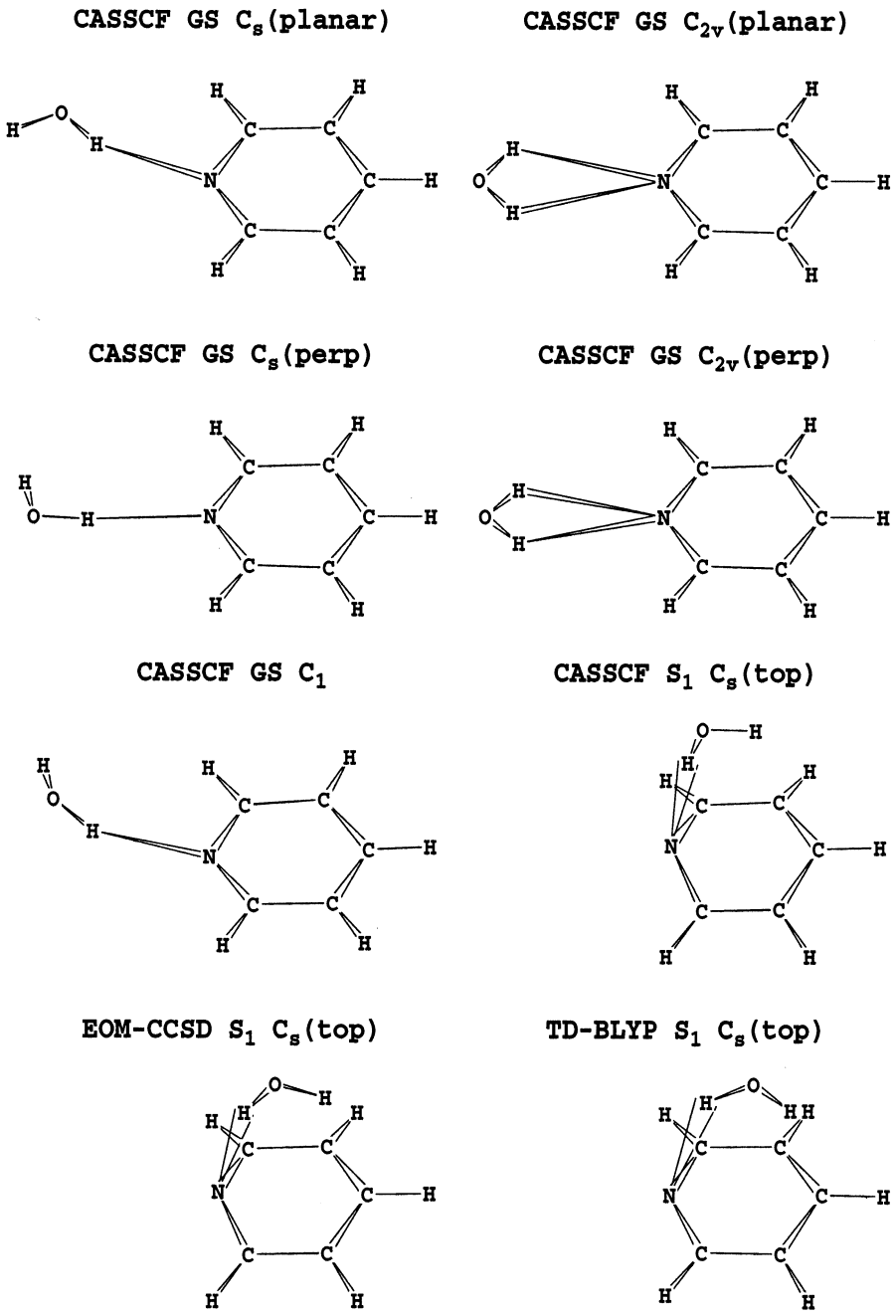

Figure 2. Hydrogen-bonded structures for the ground state (GS) and S_1 (n,π^*) excited state of water:pyridine.

mol^{-1}. As the harmonic approximation is used in these zero-point energy and thermal corrections and as the experimental value is obtained in solution rather than the gas phase, the observed and calculated values are in reasonable agreement.

The geometrical properties shown in Table 5 indicate that little structural changes are predicted for pyridine on hydrogen bonding, but as expected, significant lengthening of the OH donor bonds are found. The hydrogen-bond angles NHO and XNH (the point X is defined in Figure 1) are near 180° indicating orthodox linear hydrogen bonding. In the Supporting Information, a detailed comparison is provided between observed and calculated vibrational frequencies for the complex. In brief, one of the most important observed features is a large red shift in the hydrogen-bonded OH frequency of magnitude 270 cm^{-1} observed in matrix isolation studies[7] of water:pyridine; the calculated vibration frequencies using the cc-pVDZ basis depict red shifts at the MP2, B3LYP, and BLYP levels of 119, 162, and 178 cm^{-1}, respectively, and hence significantly underestimate the observed shift. The MP2/aug-cc-pVDZ value of 248 cm^{-1} is in good agreement with experiment, however, and hence, a systematic error is expected for all excited-state zero-point energies as for these only cc-pVDZ is used. Another significant feature is that qualitatively only rather small shifts for the vibrations of pyridine in the water:pyridine complex are observed. Although the calculations reproduce this important feature, they fail to quantitatively predict the changes to individual modes.

3.3. S_1 (n,π^*) and S_2 (π,π^*) Excited States of Water:Pyridine. Structures for the S_1 state of water:pyridine were optimized at the CASSCF, TD-BLYP, and EOM-CCSD levels using the cc-pVDZ basis set starting at the optimized C_{2v}(perp), C_{2v}(planar), and C_s(perp) structures of the ground state, and the results are shown in Table 5 (structures and fractional-BSSE-

TABLE 6: Calculated Vertical Excitation Energies (E_v) and Vertical Emission Energies (E_f), as Well as Fractional BSSE-Corrected Origin Energies (E_{00}), Predissociation Energies (E_{pre}), and Direct Vertical Dissociation Energies (E_{dir}) for Water:Pyridine Excited States, after Correction for Errors in the Calculations of Isolated Pyridine[a]

		S_1 (n,π^*)								S_2 (π,π^*)					
method	geometry	$E_f - E_f$(Py)	E_f	$E_v - E_v$(Py)	E_v	E_{dir}	E_{pre}	E_{00}	$E_{00} - E_{00}$(Py)	$E_v - E_v$(Py)	E_v	E_{dir}	E_{pre}	E_{00}	$E_{00} - E_{00}$(Py)
CASPT2	CASSCF			0.22	4.96	4.89	4.46	4.35	0.04	−0.04	4.95	5.14	4.91	4.74	−0.02
	CCSD[b]	−0.28	3.48	0.24	4.98	4.91	4.48	4.32	0.01	0.01	5.00	5.18	4.95	4.74	−0.02
EOM-CCSD	CASSCF			0.18	4.92	4.90	4.47	4.38	0.07	−0.03	4.96	5.15	4.92	4.75	−0.01
	CCSD[b]	−0.28	3.48	0.19	4.93	4.94	4.51	4.37	0.06	0.04	5.03	5.23	5.00	4.78	0.02
TD-B3LYP	CASSCF			0.21	4.95	4.89	4.46	4.50	0.19	0.01	5.00	5.14	4.91	4.74	−0.02
	CCSD[b]	−0.25	3.51	0.16	4.90	4.92	4.49	4.50	0.19	0.04	5.03	5.18	4.95	4.75	−0.01
pyridine monomer[d]			3.76		4.74			4.31			4.99			4.76	

[a] Geometries optimized using the cc-pVDZ basis set; energies determined using aug-cc-pVDZ. [b] EOM-CCSD for excited states. [c] TD-BLYP for excited states. [d] Vertical absorption and fluorescence energies from ref 61, 0−0 from ref 62.

corrected interaction energies), Figure 2 (structures), and the Supporting Information (complete description, analysis of frequency changes by mode). Analogous results for the S_2 state optimized using CASSCF and EOM-CCSD starting at the C_s(perp) ground-state geometry are also provided. For both states, the fractional-BSSE-corrected interaction energies ΔE evaluated at these geometries using CASPT2, TD-B3LYP, and EOM-CCSD with the aug-cc-pVDZ basis are also given in Table 5. Calculations for S_1 commencing at the important C_s(perp) geometry were relatively straightforward as the reduced point-group symmetry does not result in significant interactions with other states. However, both the S_2 $^1B_2$ (π,π^*) and S_3 $^1A_2$ (n,π^*) states have $^1A''$ in the reduced point-group symmetry of the complex and, as these two states are similar in energy and their conical intersection is located nearby, they mix very strongly.

For S_1, the C_{2v}(perp) and C_{2v}(planar) structures are, by symmetry, constrained to depict bifuricated N-donor hydrogen bonds. The calculated energies for these structures are positive indicating that, for these configurations, there is no net binding in the excited state.

Optimizations commencing at the C_s(perp) minimum-energy structure of the ground state led to small changes for hydrogen bonding involving the S_2 (π,π^*) state. However, for hydrogen bonding involving the S_1 (n,π^*) state, the water molecule moved from its original orthodox linear hydrogen bonding position to one in which it lies on top of the aromatic ring, with one hydrogen orientated toward the nitrogen, as before, but the other hydrogen forming a "hydrogen bond" to the aromatic π cloud. This structure is named C_s(top) and is shown in Figure 2. Although all three computational methods used depict this phenomenon, quantitatively different structures were produced, and hence, all optimized geometries are provided in Figure 2 and Table 5. The CASSCF structure has a rather large C_4 to H distance of 3.4 Å, whereas TD-BLYP decreases this to 2.4 Å. Unfortunately, at 2.4 Å, the BSSE is very large, and it is thus clear that the aug-cc-pVDZ basis set is actually required for optimizations using TD-BLYP. EOM-CCSD predicts an intermediate structure with separation 2.8 Å, and the TD-B3LYP, CASPT2, and EOM-CCSD calculations with the large basis set including fractional BSSE corrections verify that this is indeed the most realistic of the three optimized structures. At this structure, the intermolecular interaction is quite strong, with the calculated bond strengths $-\Delta E$ ranging between 5.2 and 5.7 kcal mol^{-1}. After zero-point energy (see Table 3) and thermal correction, the calculated enthalpies of formation are in the range of 4.0−4.5 kcal mol^{-1}, 70−80% of those for the hydrogen-bonding interaction in the ground state.

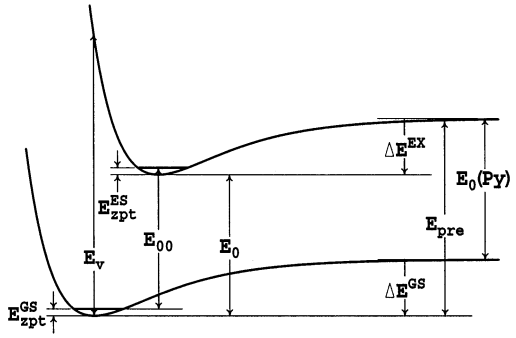

Figure 3. Schematic potential-energy surfaces for the ground state (GS) and an excited state (ES) of water:pyridine as a function of some dissociative intermolecular coordinate, indicating the adiabatic excitation energy of pyridine monomer, E_0(Py), the vertical, adiabatic, and origin transition energies of the complex, E_v, E_0, and E_{00}, respectively, the zero-point energies, E^{GS}_{zpt} and E^{ES}_{zpt}, and the hydrogen-bond interaction energies ΔE^{GS} and ΔE^{ES}.

In Table 6 is shown a variety of deduced energetic parameters for the S_1 and S_2 excited states of water:pyridine. The quantities involved are sketched in Figure 3 and include the appropriate zero-point energies E_{zpt}, interaction energies ΔE, complex vertical (E_v), adiabatic (E_0), and origin (E_{00}) transition energies, as well as the adiabatic transition energy in isolated pyridine, E_0(Py). This figure is sketched along an idealized coordinate which moves from the linear hydrogen-bonded structure of the ground state through the "top" structure of the excited state and on to molecular dissociation. The excited-state minimum is indeed accessible without barrier from the ground-state geometry, as indicated qualitatively in the figure; there are, of course, more direct paths leading to dissociation than the one which is indicated. In addition, two other energies provide indicators of the types of dynamics likely on the excited-state potential-energy surface. These are the predissociation energy

$$E_{pre} = E_{00}(\text{Py}) - \Delta E^{GS} - \Delta E^{GS}_{zpt} \quad (4)$$

which specifies the minimum energy for optical excitation that could possibly lead to dissociation of the complex in the excited state, where ΔE^{GS}_{zpt} is the change in zero-point energy due to complex formation in its ground electronic state. For dissociation to occur at this excitation energy, all energy imparted into vibrational motions of the pyridine molecule must be converted to translational energy of the fragments, however. This energy is also indicated on Figure 3; the second energy is that required for direct dissociation *without* the need for energy transfer from the excited vibrations of pyridine. As this energy is dependent on the specific vibronic level of the complex which is excited,

we consider only excitation at the band center and express the band-center direct dissociation energy as

$$E_{dir} = E_v(Py) - \Delta E^{GS} - \Delta E^{GS}_{zpt} \quad (5)$$

Table 6 provides best estimate predictions of the actual molecular properties by correcting the computed transition energies for the known errors of each particular method in predicting the transition energies of isolated pyridine. In this fashion, E_v and E_{00} for the complex are evaluated by adding to the calculated value of $E_v - E_v(Py)$ the observed value for $E_v(Py)$, etc.

For the S_1 (n,π^*) state, the calculations indicate that the predissociation energy E_{pre} of the complex is in excess of the 0−0 energy E_{00} for the top structure, and hence, this structure is predicted to provide a bound excited-state complex. The vertical excitation energy E_v from the ground-state is, however, predicted to exceed the dissociation energy by ca. 0.5 eV, and hence, it is not possible to produce water:pyridine in its excited state by irradiating the gas-phase complex. Further, the vertical excitation energy is predicted to be very close to the direct dissociation energy E_{dir}. Hence, energy transfer from intramolecular to intermolecular motions is not required in order for the vertically excited complex to predissociate, and hence, the dissociation process is expected to be very rapid.

Quite a different scenario is predicted for the S_2 (π,π^*) state. Small changes in the vertical and adiabatic transition energies are predicted upon complex formation, as is observed.[4] The vertical excitation energy E_v is intermediate between the predissociation energy E_{pre} and the direct dissociation energy E_{dir}. Hence, after vertical excitation, the complex has sufficient energy to dissociate, but energy must be transferred from the intramolecular modes to the intermolecular ones, and hence, the complex may be long-lived.

The calculated solvent shifts $E_v - E_v(Py)$ themselves are, from Table 6, on the order of 0.16−0.24 eV for the S_1 (n,π^*) state and −0.04 to +0.04 eV for the S_2 (π,π^*) one. These results are in excellent agreement with those obtained by Del Bene in her pioneering studies[17,18] of excited-state hydrogen bonding. As shown in Figure 3, the blue shift of the (n,π^*) band is indicative of the energy required to break the ground-state hydrogen bond. In aqueous solution, the (n,π^*) band is blue-shifted by at least 0.25 eV to become obscured by the intense (π,π^*) band. Our simulations of the liquid[27] indicate that the structure of the liquid is important in determining the observed solvent shift but that the value predicted for the dimeric complex is indicative of the overall effect. Also shown in Table 6 are calculated fluorescence band-maximum shifts $E_f - E_f(Py)$. For the (n,π^*) state, these indicate large shifts of −0.25 to −0.28 eV, with the reduced emission energies arising largely from the need to break the on-top hydrogen bond during the emission process. An experimental value for pyridine is not available, but corresponding values for the diazines are typically a factor of 4 smaller than this.[4,25,28,29,100] Molecular-mechanics potential surfaces for the excited state also predict the occurrence of the top structure[27] with solvent shifts of around −0.25 eV. However, the prevalence of this structure in liquid solution is quite sensitive to the details of the potential-energy surface and the precise value of the hydrogen-bond strength.

For the S_2 (π,π^*) state, the calculated origin shifts $E_{00} - E_{00}(py)$ are quite small, ranging from −0.02 to +0.02 eV (see Table 6), so that the calculated interaction energies (see Table 5) are very similar to those of the ground state. Stronger solvation of S_2 rather than S_1 raises the possibility that for the complex the lowest-lying singlet excited state is S_2 rather than S_1. Our calculated origin energies shown in Table 6 indicate that the solvation of S_1 is sufficient for it to remain lower in energy by 0.3 eV, however. Also, it is possible that the forbidden S_3 state is solvated preferentially compared to S_1 and forms the lowest-energy excited state of the complex. Although our calculations were unable to optimize the structure of S_3, no suggestions of preferential solvation of this state were found.

4. Conclusions

The failure to detect azine−water complexes after excitation to excited states[14] and the absence of fluorescence spectra shifts in solution[4] has been interpreted as indicating that hydrogen bonding does not form to the (n,π^*) excited states of azines. Here, we consider the simplest azine, pyridine, a monofunctional molecule for which no questions arise as to the localization/delocalization of the (n,π^*) excitation over different chromophores. The calculations, however, indicate that excited-state hydrogen bonding is much more complex than has previously been considered. According to expectations, the linear hydrogen bonding arrangement that forms a signature of ground-state hydrogen bonding is lost. However, an alternate paradigm for hydrogen bonding is found, one in which hydrogen bonding to aromatic rings is enhanced through the presence of excess π electron density after the (n,π^*) excitation. In fact, the calculations predict that this alternate paradigm for excited-state hydrogen bonding is only slightly weaker than the orthodox ground-state hydrogen bonding found in azine−water systems. Dissociation of water:pyridine following vertical excitation thus occurs not because there is no hydrogen bonding allowed in the excited state but rather because it provides a large amount of excess vibrational energy to the complex, an amount large enough to overcome the significant excited-state hydrogen bond strength. The failure to observe signals in two-color time-of-flight mass spectroscopic studies of diazine−water complexes[14,15] is usually interpreted in terms of the dissociative excited-state surfaces akin to that of water:pyridine. This study raises an alternate possibility, that the spectrum is not seen because of the Franck−Condon factors being small and line-broadening being large as a result of direct excited-state isomerization to top-bonded structures.

To our knowledge, the only previous study of the structure of a hydrogen bond to a molecule in an (n,π^*) excited state is that of Del Bene et al.[42] for HF and H_2CO. In this case, the hydrogen bond changes from linear to oxygen in the ground state to geometries bonded to both O (strong) and C (weak) which reflect sp^3 hybridization of the acceptor atoms. Our C_s(top) structure can be thought of as being a distorted form of the hydrogen bond to (nitrogen) sp^3 lone-pair motif seen therein. However, the clear involvement of both water hydrogens in interactions with the pyridyl π system, and the significant distortion from the sp^3 geometry, indicate that hydrogen-bonding to aromatic (n,π^*) systems in excited states provides a distinctly different motif to hydrogen-bonding involving localized π^* orbitals.

Acknowledgment. We thank the Australian Research Council for funding this research.

Supporting Information Available: Analysis of the calculated and observed frequency changes on formation of water:pyridine in its ground and excited electronic states, along with the calculated intermolecular vibration frequencies. All optimized structures, vibration frequencies, and normal modes for

the complex and its constituents. This material is available free of charge via the Internet at http://pubs.acs.org.

References and Notes

(1) Rablen, P. R.; Lockman, J. W.; Jorgensen, W. L. *J. Phys. Chem. A* **1998**, *102*, 3782.

(2) Jeffrey, G. A.; Saenger, W. *Hydrogen bonding in biological structure*; Springer-Verlag: Berlin, 1991.

(3) Baker, E. N.; Hubbard, R. E. *Prog. Biophys. Mol. Biol.* **1984**, *44*, 97.

(4) Baba, H.; Goodman, L.; Valenti, P. C. *J. Am. Chem. Soc.* **1966**, *88*, 5410.

(5) Mctigue, P.; Renowden, P. V. *J. Chem. Soc., Faraday Trans. I* **1975**, 1784.

(6) Maes, G.; Smets, J. *J. Mol. Struct.* **1992**, *270*, 141.

(7) Destexhe, A.; Smets, J.; Adamowicz, L.; Maes, G. *J. Phys. Chem.* **1994**, *98*, 1506.

(8) Zoidis, E.; Yarwood, J.; Danten, Y.; Besnard, M. *Mol. Phys.* **1995**, *85*, 373.

(9) Zoidis, E.; Yarwood, J.; Danten, Y.; Besnard, M. *Mol. Phys.* **1995**, *85*, 385.

(10) Buyl, F.; Smets, J.; Maes, G.; Adamowicz, L. *J. Phys. Chem.* **1995**, *99*, 14967.

(11) Szezepaniak, K.; Chabrier, P.; Person, W. B.; Del Bene, J. E. *J. Mol. Struct.* **1997**, *436*−*7*, 367.

(12) Mccarthy, W.; Smets, J.; Adamowicz, L.; Plokhotzichenos, A. M.; Radchenko, E. D.; Shenia, G. G.; Stepanian, S. G. *Mol. Phys.* **1997**, *91*, 513.

(13) Del Bene, J. E.; Person, W.; Szczepaniak, K. *Mol. Phys.* **1996**, *89*, 47.

(14) Wanna, J.; Menapace, J. A.; Bernstein, E. R. *J. Chem. Phys.* **1986**, *85*, 1795.

(15) Wanna, J.; Bernstein, E. R. *J. Chem. Phys.* **1987**, *86*, 6707.

(16) Del Bene, J. E. *J. Am. Chem. Soc.* **1975**, *97*, 5330.

(17) Del Bene, J. E. *Chem. Phys.* **1976**, *15*, 463.

(18) Del Bene, J. E. *Chem. Phys.* **1980**, *50*, 1.

(19) Del Bene, J. E. *J. Phys. Chem.* **1994**, *98*, 5902.

(20) Chaban, G. M.; Gordon, M. S. *J. Phys. Chem. A* **1999**, *103*, 185.

(21) Organero, J. A.; Douhal, A.; Santos, L.; Martinez-Ataz, E.; Guallar, V.; Moreno, M.; Lluch, J. M. *J. Phys. Chem. A* **1999**, *103*, 5301.

(22) McRae, E. G. *J. Phys. Chem.* **1957**, *61*, 562.

(23) Liptay, W. *Z. Naturforsch. Teil. A* **1965**, *20*, 272.

(24) Rettig, W. *J. Mol. Struct.* **1982**, *84*, 303.

(25) Zeng, J.; Hush, N. S.; Reimers, J. R. *J. Chem. Phys.* **1993**, *99*, 1508.

(26) Zeng, J.; Craw, J. S.; Hush, N. S.; Reimers, J. R. *J. Chem. Phys.* **1993**, *99*, 1482.

(27) Zeng, J.; Craw, J. S.; Hush, N. S.; Reimers, J. R. *Chem. Phys. Lett.* **1993**, *206*, 323.

(28) Zeng, J.; Woywod, C.; Hush, N. S.; Reimers, J. R. *J. Am. Chem. Soc.* **1995**, *117*, 8618.

(29) Zeng, J.; Hush, N. S.; Reimers, J. R. *J. Phys. Chem.* **1996**, *100*, 9561.

(30) Zeng, J.; Hush, N. S.; Reimers, J. R. *J. Chem. Phys.* **1993**, *99*, 1495.

(31) Kleier, D. A.; Martin, R. L.; Wadt, W. R.; Moomaw, W. R. *J. Am. Chem. Soc.* **1982**, *104*, 60.

(32) Carrabba, M. M.; Kenny, J. E.; Moomaw, W. R.; Cordes, J.; Denton, M. *J. Phys. Chem.* **1985**, *89*, 674.

(33) Jorgensen, W. L.; McDonald, N. A. *J. Mol. Struct. (THEOCHEM)* **1988**, *424*, 145.

(34) Spoliti, M.; Bencivenni, L.; Ramondo, F. *THEOCHEM* **1994**, *1994*, 185.

(35) Smets, J.; Adamowicz, L.; Maes, G. *J. Mol. Struct.* **1994**, *322*, 113.

(36) Martoprawiro, M. A.; Bacskay, G. B. *Mol. Phys.* **1995**, *85*, 573.

(37) Maes, G.; Smets, J.; Adamowicz, L.; McCarthy, W.; Van Bael, M. K.; Houben, L.; Shoone, K. *J. Mol. Struct.* **1997**, *410*−*411*, 315.

(38) Samanta, U.; Chakrabarti, P.; Chandrasekhar, J. *J. Phys. Chem. A* **1998**, *102*, 8964.

(39) Smets, J.; McCarthy, W.; Maes, G.; Adamowicz, L. *J. Mol. Struct.* **1999**, *476*, 27.

(40) Dkhissi, A.; Adamowicz, L.; Maes, G. *J. Phys. Chem. A* **2000**, *104*, 2112.

(41) Papai, I.; Jancso, G. *J. Phys. Chem. A* **2000**, *104*, 2132.

(42) Del Bene, J. E.; Gwaltney, S. R.; Bartlett, R. J. *J. Phys. Chem. A* **1998**, *102*, 5124.

(43) Hush, N. S.; Reimers, J. R. *Coord. Chem. Rev.* **1998**, *177*, 37.

(44) Gregory, J.; Clary, D. C. *Mol. Phys.* **1996**, *88*, 33.

(45) Fredericks, S. Y.; Jordan, K. D.; Zwier, T. S. *J. Phys. Chem.* **1996**, *100*, 7810.

(46) Tarakeshwar, P.; Kim, K. S.; Brutschy, B. *J. Chem. Phys.* **1999**, *110*, 8501.

(47) Bauernschmitt, R.; Ahlrichs, R. *Chem. Phys. Lett.* **1996**, *256*, 454.

(48) Bauernschmitt, R.; Häser, M.; Treutler, O.; Ahlrichs, R. *Chem. Phys. Lett.* **1997**, *264*, 573.

(49) Casida, M. E.; Jamorski, C.; Casida, C. K.; Salahub, D. R. *J. Chem. Phys.* **1998**, *108*, 4439.

(50) Stratmann, R. E.; Scuseria, G. E.; Frisch, M. J. *J. Chem. Phys.* **1998**, *109*, 8218.

(51) van Gisbergen, S. J. A.; Kootstra, F.; Schipper, P. R. T.; Gritsenko, O. V.; Snijders, J. G.; Baerends, E. J. *Phys. Rev. A* **1998**, *57*, 2556.

(52) Tozer, D. J.; Amos, R. D.; Handy, N. C.; Roos, B. O.; Serrano-Andrés, L. *Mol. Phys.* **1999**, *97*, 859.

(53) Becke, A. D. *J. Chem. Phys.* **1993**, *98*, 5648.

(54) Lee, C.; Yang, W.; Parr, R. G. *Phys. Rev. B* **1988**, *37*, 789.

(55) Becke, A. D. *Phys. Rev. A* **1988**, *38*, 3098.

(56) Møller, C.; Plesset, M. S. *Phys. Rev. A* **1934**, *46*, 618.

(57) Hegarty, D.; Robb, M. A. *Mol. Phys.* **1979**, *38*, 1795.

(58) Andersson, K.; Malmqvist, P.-Å.; Roos, B. O. *J. Chem. Phys.* **1992**, *96*, 1218.

(59) Purvis, G. D., III; Bartlett, R. J. *J. Chem. Phys.* **1982**, *76*, 1910.

(60) Stanton, J. F.; Bartlett, R. J. *J. Chem. Phys.* **1993**, *98*, 7029.

(61) Cai, Z.-L.; Reimers, J. R. *J. Phys. Chem. A* **2000**, *104*, 8389.

(62) Innes, K. K.; Ross, I. G.; Moomaw, W. R. *J. Mol. Spectrosc.* **1988**, *132*, 492.

(63) Innes, K. K.; Byrne, J. P.; Ross, I. G. *J. Mol. Spectrosc.* **1967**, *22*, 125.

(64) Jesson, J. P.; Kroto, H. W.; Ramsay, D. A. *J. Chem. Phys.* **1972**, *56*, 6257.

(65) Mochizuki, Y.; Kaya, K.; Ito, M. *J. Phys. Chem.* **1978**, *69*, 935.

(66) Dilella, D. P.; Stidham, H. D. *J. Raman Spectrosc.* **1980**, *9*, 90.

(67) Stidham, H. D.; DiLella, D. P. *J. Raman Spectrosc.* **1980**, *9*, 247.

(68) Bolovinos, A.; Tsekeris, P.; Philis, J.; Phantos, E.; Andritsopoulos, G. *J. Mol. Spectrosc.* **1984**, *103*, 240.

(69) Villa, E.; Amirav, A.; Lim, E. C. *J. Phys. Chem.* **1988**, *92*, 5393.

(70) Walker, I. C.; Palmer, M. H.; Hopkirk, A. *Chem. Phys.* **1989**, *141*, 365.

(71) Destexhe, A.; Dsmets, J.; Adamowicz, L.; Maes, G. *J. Phys. Chem.* **1994**, *98*, 1506.

(72) Becucci, M.; Lakin, N. M.; Pietraperzia, G.; Salvi, P. R.; Castellcui, E.; Kerstel, E. R. Th. *J. Chem. Phys.* **1997**, *107*, 10399.

(73) Chachisvilis, M.; Zewail, A. H. *J. Phys. Chem. A* **1999**, *103*, 7408.

(74) Foresman, J. B.; Head-Gordon, M.; Pople, J. A.; Frisch, M. J. *J. Phys. Chem.* **1992**, *96*, 135.

(75) Lorentzon, L.; Fülscher, M. P.; Roos, B. O. *Theor. Chim. Acta* **1995**, *92*, 67.

(76) Martin, J. M. L.; Van Alsenoy, C. *J. Phys. Chem.* **1996**, *100*, 6973.

(77) Del Bene, J. E.; Watts, J. D.; Bartlett, R. J. *J. Chem. Phys.* **1997**, *106*, 6051.

(78) Nooijen, M.; Bartlett, R. J. *J. Chem. Phys.* **1997**, *106*, 6441.

(79) Ahlrichs, R.; Bär, M.; Baron, H.-P.; Bauernschmitt, R.; Böcker, S.; Ehrig, M.; Eichkorn, K.; Elliot, S.; Haase, F.; Häser, M.; Horn, H.; Huber, C.; Huniar, U.; Kattannek, M.; Kölmel, C.; Kollwitz, M.; Ochsenfeld, C.; Öhm, H.; Schäfer, A.; Schneider, U.; Treutler, O.; von Arnim, M.; Weigend, F.; Weis, P.; Weiss, H. *TURBOMOLE*; Quantum Chemistry Group: University of Karlsruhe, 1997, Version 4.

(80) Eichkorn, K.; Treutler, O.; Öhm, H.; Häser, M.; Ahlrichs, R. *Chem. Phys. Lett.* **1995**, *242*, 652.

(81) Frisch, M. J.; Trucks, G. W.; Schlegel, H. B.; Scuseria, G. E.; Robb, M. A.; Cheeseman, J. R.; Zakrzewski, V. G.; Montgomery, J. A., Jr.; Stratmann, R. E.; Burant, J. C.; Dapprich, S.; Millam, J. M.; Daniels, A. D.; Kudin, K. N.; Strain, M. C.; Farkas, O.; Tomasi, J.; Barone, V.; Cossi, M.; Cammi, R.; Mennucci, B.; Pomelli, C.; Adamo, C.; Clifford, S.; Ochterski, J.; Petersson, G. A.; Ayala, P. Y.; Cui, Q.; Morokuma, K.; Malick, D. K.; Rabuck, A. D.; Raghavachari, K.; Foresman, J. B.; Cioslowski, J.; Ortiz, J. V.; Stefanov, B. B.; Liu, G.; Liashenko, A.; Piskorz, P.; Komaromi, I.; Gomperts, R.; Martin, R. L.; Fox, D. J.; Keith, T.; Al-Laham, M. A.; Peng, C. Y.; Nanayakkara, A.; Gonzalez, C.; Challacombe, M.; Gill, P. M. W.; Johnson, B. G.; Chen, W.; Wong, M. W.; Andres, J. L.; Head-Gordon, M.; Replogle, E. S.; Pople, J. A. *Gaussian 98*, revision A.7; Gaussian, Inc.: Pittsburgh, PA, 1998.

(82) Stanton, J. F.; Gauss, J.; Watts, J. D.; Nooijen, M.; Oliphant, N.; Perera, S. A.; Szalay, P. G.; Lauderdale, W. J.; Gwaltney, S. R.; Beck, S.; Balková, A.; Bernholdt, D. E.; Baeck, K.-K.; Rozyczko, P.; Sekino, H.; Hober, C.; Bartlett, R. J. *ACES II* a product of the Quantum Theory Project; University of Florida: Gainsville, FL, 1999.

(83) Helgaker, T.; Jensen, H. J. Aa.; Joergensen, P.; Olsen, J.; Ruud, K.; Aagren, H.; Andersen, T.; Bak, K. L.; Bakken, V.; Christiansen, O.; Dahle, P.; Dalskov, E. K.; Enevoldsen, T.; Fernandez, B.; Heiberg, H.; Hettema, H.; Jonsson, D.; Kirpekar, S.; Kobayashi, R.; Koch, H.; Mikkelsen, K. V.; Norman, P.; Packer, M. J.; Saue, T.; Taylor, P. R.; Vahtras, O. *Dalton*, release 1.0; University of Oslo: Oslo, Norway, 1997.

(84) Andersson, K.; Blomberg, M. R. A.; Fülscher, M. P.; Karlström, G.; Lindh, R.; Malmqvist, P. -Å.; Neogrády, P.; Olsen, J.; Roos, B. O.;

Sadlej, A. J.; Seijo, L.; Serrano-Andrés, L.; Siegbahn, P. E. M.; Widmark, P.-O. *Molcas*, version 4; University of Lund: Lund, Sweden, 1997.

(85) Werner, H.-J.; Knowles, P. J.; Amos, R. D.; Bernhardsson, A.; Berning, A.; Celani, P.; Cooper, D. L.; Deegan, M. J. O.; Hampel, C.; Lindh, R.; Lloyd, A. W.; Meyer, W.; Nicklass, A.; Peterson, K.; Pitzer, R.; Stone, A. J.; Taylor, P. R.; Mura, M. E.; Pulay, P.; Schütz, M.; Stoll, H.; Thorsteinsson, T. *MOLPRO-2000*; University of Birmingham: Birmingham, U.K., 2000.

(86) Dunning, T. H., Jr. *J. Chem. Phys.* **1989**, *90*, 1007.

(87) Kendall, R. A.; Dunning, T. H., Jr.; Harrison, R. J. *J. Chem. Phys.* **1992**, *96*, 6796.

(88) Boys, S. F.; Benardi, F. *Mol. Phys.* **1970**, *19*, 553.

(89) Van Duijneveldt, F. B.; Van Duijnevldt-van de Rijdt, G. C.; van Leuthe, J. H. *Chem. Rev.* **1994**, *94*, 1973.

(90) Dunning, T. H., Jr. *J. Phys. Chem. A* **2000**, *104*, 9062.

(91) Lambropoulos, N. A.; Reimers, J. R.; Hush, N. S. *J. Chem. Phys.* **2002**, *116*, 10277.

(92) Scott, A. P.; Radom, L. *J. Phys. Chem.* **1996**, *100*, 16502.

(93) Hoy, A. R.; Bunker, P. B. *J. Mol. Spectrosc.* **1974**, *74*, 1.

(94) Herzberg, G. *Molecular spectra and molecular structure. III. Electronic spectra and electronic structure of polyatomic molecules*; D. Van Nostrand: Princeton, NJ, 1966.

(95) Buma, W. J.; Groenen, E. J. J.; Schmidt, J.; de Beer, R. *J. Chem. Phys.* **1989**, *91*, 6549.

(96) Martin, J. M. L. *Chem. Phys. Lett.* **1966**, *259*, 669.

(97) Wood, D. E.; Dunning, T. H., Jr. *J. Chem. Phys.* **1993**, *99*, 1914.

(98) Cai, Z.-L.; François, J. P. *Chem. Phys. Lett.* **1999**, *300*, 69.

(99) McTigue, P.; Renowden, P. V. *J. Chem. Soc., Faraday Trans. I* **1975**, 1784.

(100) Hush, N. S.; Reimers, J. R. *Chem. Rev.* **2000**, *100*, 775.